

# Coherent Audio-Visual Editing via Conditional Audio Generation Following Video Edits

Masato Ishii<sup>1</sup>Akio Hayakawa<sup>1</sup>Takashi Shibuya<sup>1</sup>Yuki Mitsufuji<sup>1,2</sup><sup>1</sup>Sony AI<sup>2</sup>Sony Group Corporation

{Masato.A.Ishii, Akio.Hayakawa, Takashi.Tak.Shibuya, Yuhki.Mitsufuji}@sony.com

## Abstract

We introduce a novel pipeline for joint audio-visual editing that enhances the coherence between edited video and its accompanying audio. Our approach first applies state-of-the-art video editing techniques to produce the target video, then performs audio editing to align with the visual changes. To achieve this, we present a new video-to-audio generation model that conditions on the source audio, target video, and a text prompt. We extend the model architecture to incorporate conditional audio input and propose a data augmentation strategy that improves training efficiency. Furthermore, our model dynamically adjusts the influence of the source audio based on the complexity of the edits, preserving the original audio structure where possible. Experimental results demonstrate that our method outperforms existing approaches in maintaining audio-visual alignment and content integrity.

## 1. Introduction

Recent advancements in video editing have enabled sophisticated manipulation of visual content [25, 26]. However, these techniques typically address only the visual modality, overlooking the crucial role of audio in most real-world videos. As a result, there is a growing demand for editing solutions that maintain strong audio-visual coherence. The emergence of audio-visual generation models, such as Veo 3 [8] and Sora 2 [42], underscores the increasing importance of synchronized audio and video in content creation.

Existing approaches to joint audio-video editing face significant limitations. Editing audio and video modalities independently often results in poor alignment, as changes in one stream may not correspond to changes in the other. Alternatively, applying video-to-audio models to edited videos can disrupt the integrity of the original audio. To address these issues, joint editing methods have been studied [32, 33], but they are restricted to low frame-rate videos (e.g., 4 fps [33]), which is impractical for most applica-

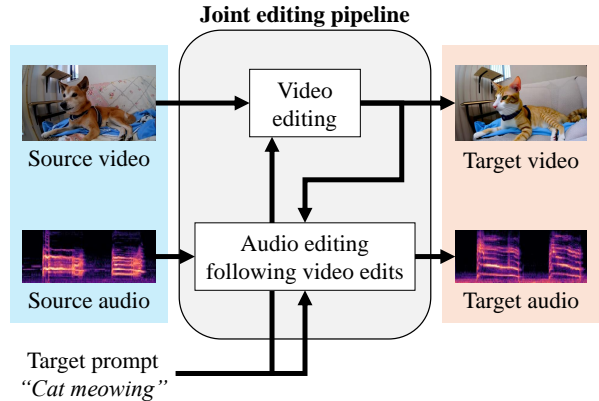


Figure 1. An overview of the proposed pipeline.

tions. In contrast, modern video editing methods can process much higher frame rates (e.g., 16 fps [25]), but lack integrated audio editing capabilities.

To address these challenges, we propose a new pipeline for joint audio-visual editing. As shown in Fig. 1, our method first utilizes advanced video editing techniques to create the target video, and then employs a novel video-to-audio generation model, which is conditioned on the source audio, target video, and a text prompt to edit the audio in alignment with the visual changes. We enhance the model architecture of the latest video-to-audio model [5] to accept conditional audio input and introduce a data augmentation strategy for the new conditional input to improve training efficiency. Importantly, our model dynamically adjusts the influence of the source audio based on the complexity of the edits, maximizing preservation of the original audio structure. This approach leverages the strengths of state-of-the-art video editing while ensuring high audio-visual alignment. Experimental results demonstrate that our pipeline achieves superior performance compared to existing methods, particularly in maintaining audio-visual alignment and content integrity.

## 2. Preliminaries and related work

### 2.1. Flow matching

Flow matching [34] is a framework for generative modeling that has been widely adopted across various domains due to its strong performance and high scalability. It employs a strategy essentially similar to diffusion models [21] but offers greater flexibility in model design [14]. In this framework, the model learns a time-dependent velocity field. Let  $\mathbf{x}_0$  and  $\mathbf{x}_1$  denote samples from the prior and target distributions, respectively, and define  $\mathbf{x}_t = t\mathbf{x}_0 + (1-t)\mathbf{x}_1$  as the linear interpolation between them at time  $t \in [0, 1]$ . The model  $u_\theta(\mathbf{x}, t)$ , parameterized by  $\theta$ , predicts the velocity at each time  $t$ .

The model is trained by minimizing the conditional flow-matching objective:

$$\min_{\theta} \mathbb{E}_{p(\mathbf{x}_0), p(\mathbf{x}_1), \mathcal{U}(t)} \|u_\theta(\mathbf{x}_t, t) - u(\mathbf{x}_t | \mathbf{x}_0, \mathbf{x}_1)\|^2, \quad (1)$$

where  $u(\mathbf{x}_t | \mathbf{x}_0, \mathbf{x}_1)$  is the conditional velocity. In the current setting, where  $\mathbf{x}_t$  is defined as a linear interpolation between  $\mathbf{x}_0$  and  $\mathbf{x}_1$ , the conditional velocity simplifies to  $u(\mathbf{x}_t | \mathbf{x}_0, \mathbf{x}_1) = \mathbf{x}_1 - \mathbf{x}_0$ .

Given a trained flow-matching model, we can define the following ordinary differential equation (ODE):

$$\frac{d\mathbf{x}_t}{dt} = u_\theta(\mathbf{x}_t, t). \quad (2)$$

By solving this ODE from  $t = 0$  (with initial sample  $\mathbf{x}_0 \sim p(\mathbf{x}_0)$ ) to  $t = 1$ , we can transform a sample from the prior distribution into a sample from the target distribution  $p(\mathbf{x}_1)$ . By choosing a tractable distribution (e.g., Gaussian) for  $p(\mathbf{x}_0)$  and the target data distribution for  $p(\mathbf{x}_1)$ , this model can serve as a generative model.

When modeling conditional generation, the model is extended to accept a conditional input  $\mathbf{C}$ , resulting in  $u_\theta(\mathbf{x}_t, t, \mathbf{C})$ , and the training objective in Eq. (1) is modified to sample from the joint distribution  $p(\mathbf{x}_1, \mathbf{C})$  instead of  $p(\mathbf{x}_1)$ . During inference, classifier-free guidance [20] can be applied to the velocity prediction to improve fidelity to the given condition:

$$\begin{aligned} \tilde{u}_\theta(\mathbf{x}_t, t, \mathbf{C}) &= u_\theta(\mathbf{x}_t, t, \emptyset) \\ &+ w(u_\theta(\mathbf{x}_t, t, \mathbf{C}) - u_\theta(\mathbf{x}_t, t, \emptyset)), \end{aligned} \quad (3)$$

where  $\emptyset$  represents the null condition, and  $w$  is a coefficient to control the strength of the guidance. To enable the model to handle the null condition, the conditional input is randomly dropped with a small probability (e.g., 0.1) during training.

### 2.2. Single-modal data editing

Editing refers to the process of creating target data by modifying specific content in given source data, as intended by

the user, while preserving unrelated elements. This section briefly reviews editing methods based on flow matching or diffusion models in both audio and video domains.

**Audio Editing.** Audio editing methods can be broadly categorized into training-based and training-free approaches. In the training-based approach [30, 48], models are trained as conditional generators that take source audio as input and produce edited outputs. While conceptually straightforward, this method faces significant challenges in assembling large-scale datasets of paired source and target audio samples. Our method is also training-based one, but we avoid this issue by adopting acoustic feature extraction as described in Section 3.2.

In contrast, training-free approaches [24, 38, 51] utilize pre-trained text-to-audio generation models [17, 35, 36] to generate the desired audio edits. To ensure preservation of unrelated content, these methods inject source audio information into the generation process using inversion techniques [46] and attention control [19]. Although this approach eliminates the need for training with specialized datasets, it typically incurs higher computational costs during generation.

**Video Editing.** Training video generation models is considerably more resource-intensive than audio models. As a result, most video editing methods rely on pre-trained generative models. There are two main types of pre-trained models used: text-to-image and text-to-video models.

Early work leveraged text-to-image models such as Stable Diffusion [44] due to their accessibility and ease of use. Since these models are only capable of generating single frames, specialized techniques [6, 7, 16, 26, 31] and fine-tuning strategies [37, 50] have been developed to improve temporal consistency across video frames.

Recently, the emergence of advanced text-to-video generation models [1, 47, 52] has enabled more effective video editing. Studies utilizing these models [13, 25, 45, 53] demonstrate excellent temporal consistency.

### 2.3. Joint audio-video editing

Joint audio-video editing presents unique challenges compared to single-modal editing. Editing audio and video independently often results in poor alignment between the generated modalities, degrading the overall audio-visual coherence in the edited output. Therefore, ensuring strong alignment between audio and video is a central focus in this task, and it has been addressed in only a few recent studies [32, 33].

Liang et al. [32] introduced a lightweight module that embeds the source audio-video pair into a specialized text token. This token is then input into pre-trained text-to-image and text-to-audio models to generate the correspond-

ing video frames and audio. In contrast, Lin et al. [33] extended score distillation sampling to the cross-modal setting by jointly leveraging pre-trained text-to-image and text-to-audio models. They further incorporated a contrastive loss on relevant and irrelevant regions within the audio-video pair to improve consistency between audio and video edits.

However, these approaches share two main limitations. First, they depend on text-to-image models for video editing, which restricts the ability to maintain temporal consistency across video frames. Second, they lack mechanisms to synchronize the temporal alignment between edited audio and video, making precise audio-visual alignment difficult. Thus, their application is essentially limited to low frame-rate videos (e.g., 1 fps [32] or 4 fps [33]).

In our method, we address these limitations with a sequential approach to joint editing. First, we apply a state-of-the-art video editing technique to generate the target video, ensuring high temporal consistency. Next, we use our novel video-to-audio model, which incorporates the source audio as a conditional input, to conduct audio editing following the video edits, thereby achieving strong audio-visual alignment in much higher frame-rate videos (20 fps in the experiments).

### 3. Proposed method

In this section, we first show an overview of our method and briefly explain how it works. Then, we describe the details of the newly introduced mechanisms designed for the video-guided audio editing task.

#### 3.1. Overview

Our goal is to build a model that generates edited audio aligned with the target edited video while preserving the acoustic structure of the source audio. To achieve this, we first extract hierarchical acoustic features from the source audio to capture its structural information at multiple levels of detail (Section 3.2). These features, together with conditional features from the target video and optionally a target prompt, are fed into the model (Section 3.3), which is trained to generate the edited audio using a flow matching framework. To improve training, we introduce a new data-augmentation strategy for the acoustic features called detail-temporal masking (Section 3.4). During generation, the model automatically selects the appropriate level of detail for the acoustic features based on the estimated editability score, which is determined by measuring the semantic similarity between the source audio and the target video (Section 3.5).

#### 3.2. Hierarchical acoustic feature extraction

**Motivation.** To preserve the acoustic structure of the source audio, we need to extract this information from it.

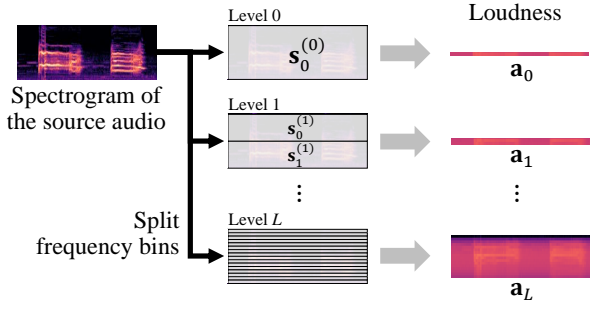


Figure 2. Hierarchical acoustic features.

In our setting, the feature representation should satisfy the following three properties:

- The feature effectively represents the acoustic structure information.
- The feature is robust to semantic changes during editing, ensuring it remains informative for generating the edited audio.
- The feature can be extracted at multiple levels of detail, enabling control over the amount of preserved structural information.

A common choice to extract audio features would be using a pretrained model. However, such a model generally does not satisfy the second property, as they are typically trained to be sensitive to differences in audio semantics (e.g., CLAP [10]). In addition, extracting semantic features at a specified level of detail is challenging, which conflicts with the third property. Consequently, we design simpler statistical features of audio signals that satisfy all three properties. Statistical features, such as loudness, are less sensitive to semantic changes in audio content, making them more reliable for preserving structural information [15].

**Implementation.** Inspired by Sketch2Sound [15], our acoustic feature is based on the frame-wise loudness of the audio signal processed with a median filter for temporal smoothing. We follow a common definition of loudness, which is an A-weighted sum across the frequency bins in a magnitude spectrogram [41]. To extract acoustic features at various levels of detail, we recursively split the frequency bins of the magnitude spectrogram into two sub-ranges (e.g., low and high frequencies) and compute the loudness for each sub-range at every level. Let  $\mathbf{s} \in \mathbb{R}^{F \times T_a}$  denote the spectrogram of the audio, where  $F$  is the number of frequency bins and  $T_a$  is the number of time-frames. At level  $l$ ,  $\mathbf{s}$  is divided into  $\{\mathbf{s}_i^{(l)} \in \mathbb{R}^{F/2^l \times T_a}\}_{i=0, \dots, 2^l-1}$ , and the acoustic features are calculated as follows:

$$\mathbf{a}_l = \text{concat} \left( \{A(\mathbf{s}_i^{(l)})\}_{i=0, \dots, 2^l-1} \right), \quad (4)$$

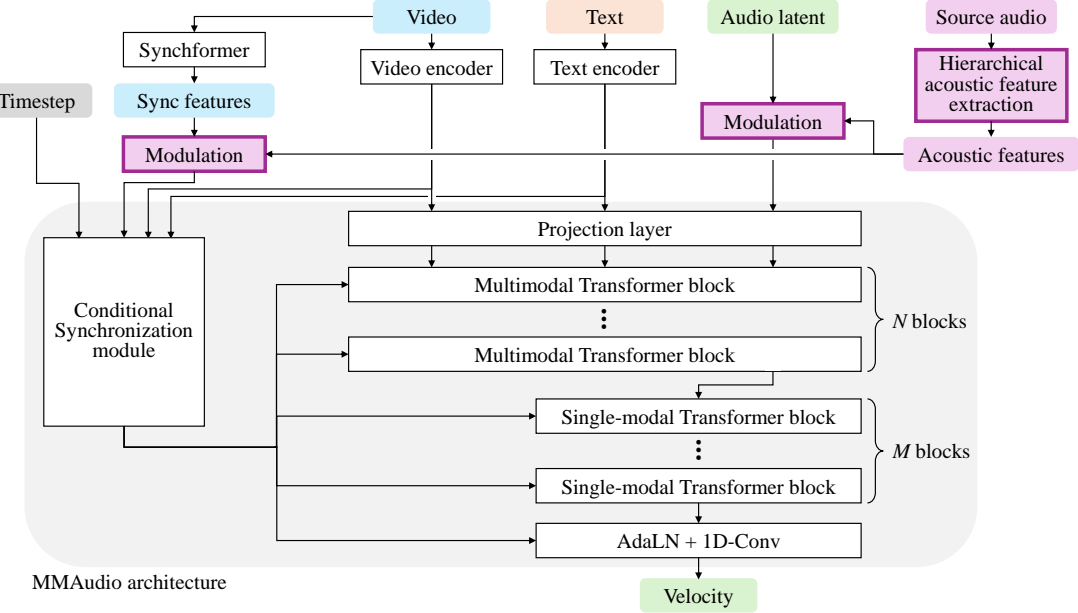


Figure 3. The architecture of our model. The major modifications from MMAudio are shown in purple.

where  $A$  is a function that computes the A-weighted sum, and concat denotes concatenation along the frequency axis.

As shown in Fig. 2, this process yields a hierarchy of acoustic features  $\{\mathbf{a}_l\}$ , from coarse to fine detail, allowing flexible control over structural information preservation. The level of detail can be controlled by masking out the features corresponding to finer details. Specifically, the acoustic features at the specified level of detail are given by:

$$\mathbf{a} = \text{concat}(\{\mathbf{a}_l \odot \mathbf{m}_l, \mathbf{m}_l\}_{l=0, \dots, L}), \quad (5)$$

where  $L$  is the maximum level, and  $\mathbf{m}_l \in \mathbb{R}^{2^l \times T_a}$  denote a mask at level  $l$ , whose elements are all zero if  $l$  is larger than the specified level, and all one otherwise. In the remainder of this paper, we refer to  $\mathbf{a}$ , consisting of the hierarchical loudness features and their corresponding mask (which specifies the level of detail), as the acoustic features.

### 3.3. Model architecture

Our model is based on the MMAudio architecture [5], with two key modifications to effectively handle information from the acoustic features during the generation process.

**Base architecture.** The backbone of the base model is a multi-modal Transformer that processes noisy audio latents, as well as conditional text and video features, to predict the velocity for audio generation through the flow matching framework. Following the latest text-to-image models [29], it comprises a sequence of MM-DiT blocks [11] followed by a sequence of audio-only single-modal DiT blocks. Additionally, the base model includes

a conditional synchronization module to enhance audio-visual synchrony. This module extracts high frame-rate features from the input video using Syncformer [23] and combines them with temporally-global conditional features extracted from text and video. The combined features are fed into the DiT blocks through adaptive layer normalization [43].

**Modifications.** To incorporate the acoustic features, we introduce two modifications to the base model:

- **Modulation of audio latents:** We add the processed acoustic features to the audio latents. Before the addition, we adjust the temporal length of the acoustic features by linear interpolation and process them with a trainable linear layer to match the dimensionality of the audio latents. This approach, which uses input addition or concatenation, is a common method for integrating conditional structural data into flow matching models and has been widely used in prior studies such as Wang et al. [49] and Zhu et al. [54].
- **Modulation of Syncformer features:** We also modulate the Syncformer features in a frame-wise manner using the acoustic features, which are processed with temporal length regulation and a feed-forward module (as used in the DiT block). This temporally-local modulation is important because the Syncformer features are used for adaptive layer normalization in the base model and thus strongly influence the generated audio in terms of temporal dynamics. To properly reflect the conditional acoustic information in the generation process, it is essen-

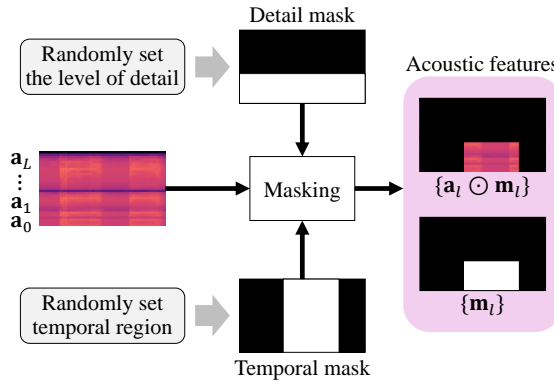


Figure 4. Detail-temporal masking of the acoustic features during training.

tial to modulate the Synchformer features before they are used in adaptive normalization.

These modules are initialized so that the modulation simply results in an identical function. During training, they are fixed in the first half of the training iterations and are set trainable there after. We adopt this two-stage training strategy to prevent the model from too much focusing on the acoustic features rather than the text prompt and the target video to generate the target audio.

### 3.4. Training with detail-temporal masking

We train our model through flow matching described in Section 2.1. Ideally, training would require sets of source audio, text prompt, target video, and target audio for each sample, but collecting such paired data with accompanying text and video at scale is challenging. Instead, we use standard text-audio-video data as a triplet of text prompt, target audio, and target video. To mimic the acoustic features of the source audio, we extract them from the target audio. Since the acoustic features are robust to semantic differences, as explained in Section 3.2, we expect the model to learn effectively from such training data.

We jointly apply two kinds of masking to augment the acoustic features as shown in Fig. 4: detail masking and temporal masking. These two masking processes are introduced for separate purposes as described below.

- **Detail masking.** For each training sample, we randomly determine the level of detail of the acoustic features. Since this corresponds to randomly choosing a proper mask for the acoustic features as described in Section 3.2, we refer to this augmentation as detail masking. The detail masking enables the model to work with various levels of details, which means that we can control how much the original acoustic structure in the source audio should be preserved in the target audio at the inference time. We also include a choice to totally mask out the entire acous-

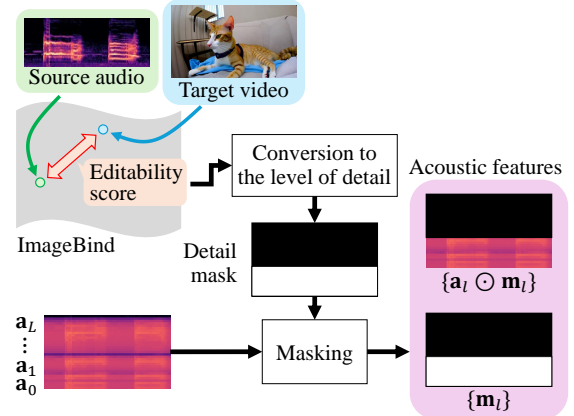


Figure 5. The adaptive conditioning based on the editability score.

tic features in the setting, allowing us to apply classifier-free guidance to our model for more accurate structure preservation.

- **Temporal masking.** We also apply random masking along with the temporal dimension to prevent the model from excessively relying on the acoustic features to generate the target audio. Since the acoustic features contain temporally rich information of the audio, especially when the level of detail is high, the model tends to focus more on aligning with the acoustic features rather than text and video. This leads to degrading text fidelity and audio-visual alignment, which is not desirable for the audio editing task. To alleviate this issue, we mask out the acoustic features at randomly selected time frames during training. It enforces the model to jointly reflect both the acoustic features and the other conditional features to generate the target audio.

### 3.5. Generation with adaptive conditioning

Once the model is trained, we can generate the target audio by solving the ODE as described in Section 2.1. Following the prior works on multi-conditional generation [2, 4, 28], we adopt classifier-free guidance with multiple guidance terms as shown below:

$$\begin{aligned} \tilde{u}_\theta(\mathbf{x}_t, t, \mathbf{C}, \mathbf{a}) = & u_\theta(\mathbf{x}_t, t, \emptyset, \emptyset) \\ & + w_1(u_\theta(\mathbf{x}_t, t, \mathbf{C}, \emptyset) - u_\theta(\mathbf{x}_t, t, \emptyset, \emptyset)) \\ & + w_2(u_\theta(\mathbf{x}_t, t, \mathbf{C}, \mathbf{a}) - u_\theta(\mathbf{x}_t, t, \mathbf{C}, \emptyset)), \end{aligned} \quad (6)$$

where  $\mathbf{a}$  and  $\mathbf{C}$  represent the acoustic features extracted from the source audio and a pair of text and video conditions, respectively, and  $w_1$  and  $w_2$  are coefficients to control the strength of two guidance terms. The first guidance term enhances the fidelity to the text and video conditioning, while the second term improves the structure preservation.

tion through referring to the acoustic features. In the experiments, we used  $w_1 = 7.5$  and  $w_2 = 0.5w_1$ .

During generation, the model adaptively selects the appropriate level of detail for the acoustic features depending on the estimated difficulty of the audio editing task. This selection is performed deterministically based on an editability score, as described below. We term this process adaptive conditioning.

**Motivation of adaptive conditioning.** The optimal level of detail for the acoustic features depends on how difficult the audio editing task is. For easy edits, where the source audio is already similar to the target (e.g., bird chirping  $\rightarrow$  seagull chirping), preserving detailed acoustic features helps maintain structural fidelity without sacrificing alignment with the target prompt and video. In contrast, for difficult edits, where significant changes are needed (e.g., cat meowing  $\rightarrow$  lion roaring), retaining too much detail from the source is less effective, much of the original acoustic structure will be altered or lost. Therefore, our method adaptively adjusts the level of acoustic detail based on the estimated editing difficulty for each sample, aiming to balance structural preservation and target fidelity.

**Implementation of adaptive conditioning.** To implement adaptive conditioning, we estimate an editability score that represents how easy the audio editing is expected to be. Specifically, we compute the audio-visual semantic similarity between the source audio and the target video. We use ImageBind [18] to embed the audio and video clips in a common feature space and then calculate the cosine similarity between these embeddings. Since ImageBind can only handle relatively short clips (e.g., two seconds), we use a sliding window approach with a window size of two seconds without overlapping, repeating this process and averaging the similarities across all time frames.

Given the editability score  $s$ , we determine the level of detail by quantizing the normalized score as shown below.

$$l = \text{round} \left( l_{\max} \cdot \text{clamp} \left( \frac{s - s_{\min}}{s_{\max} - s_{\min}} \right) \right), \quad (7)$$

where  $s_{\min}$  and  $s_{\max}$  are the expected maximum and minimum scores, respectively, and  $l_{\max}$  denote the maximum level of detail. For example, an easy edit (high similarity,  $s$  close to  $s_{\max}$ ) results in a higher level of detail being preserved, while a difficult edit (low similarity,  $s$  close to  $s_{\min}$ ) results in less detail being retained.

We control the strength of adaptive conditioning by changing the value of  $l_{\max}$ . Allowing a larger level of detail leads to more accurate preservation of the original audio structure. On the other hand, we fix both  $s_{\max}$  and  $s_{\min}$ . To determine these values, we empirically investigated the editability scores of genuine pairs of audio and

video as well as those of random pairs in the VGGSound validation dataset [3], which can be considered as the maximum and minimum levels of the editability score for this dataset. Their average scores are 0.32 and 0.02, and these are used to set  $s_{\max}$  and  $s_{\min}$ , respectively.

## 4. Experiments

### 4.1. Dataset and evaluation metrics

**Training datasets.** Following the prior work [5], we jointly used several text-video-audio and text-audio datasets to train our model: VGGSound [3], AudioCaps [27], Clotho [9], and WavCaps [39]. All audio clips were resampled to 16 kHz, and 8-second segments were cropped without overlap for each training sample.

**Evaluation dataset.** We used the AvED-Bench dataset [33], which has particularly been constructed to evaluate audio-visual editing performance. The AvED-Bench dataset consists of 110 ten-second clips covering various types of natural audio-visual events. For each clip, a pair of the source and target prompts is given to specify the editing task. Audio and video were resampled to 16 kHz and 20 fps, respectively, and used as the source audio and video in our experiments.

**Metrics.** We assess the generation quality from three different perspectives:

- **Audio-visual alignment (IB-AV)** assesses the alignment of the target audio to the target video. We used ImageBind to compute it as described in Section 3.5.
- **Structure preservation (LPAPS)** assesses how much the acoustic structure of the source audio is preserved in the target audio. Following the prior audio-editing studies [33, 38], we used LPAPS [22] to evaluate the structure preservation.
- **Text fidelity (IB-TA)** assesses the fidelity of the target audio to the given target prompt using ImageBind. Since ImageBind can only handle two-second audio clips, we cropped five non-overlapping audio sub-clips from the target audio and extracted ImageBind features from each sub-clip. Then, we computed the cosine similarity between those features and the feature extracted from the target prompt. To aggregate the multiple similarities, we used max pooling, because the audio event described in the target prompt is often temporally local (e.g., dog barking) and thus could be missed in several sub-clips.

### 4.2. Setup

We evaluated several methods representing two main approaches to audio-visual editing: independent and sequential.

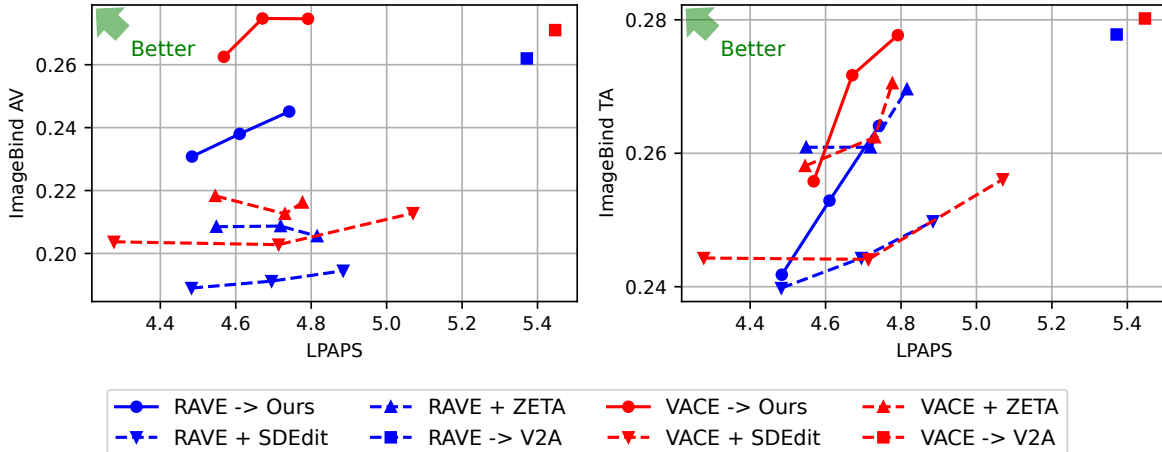


Figure 6. Experimental results on the AvED-Bench dataset. The horizontal axis represents structure preservation (lower is better). The vertical axis in the left plot indicates audio-visual alignment, while the right plot shows text fidelity (higher is better in both cases). For each method except  $\ast \rightarrow \text{V2A}$ , we varied the hyperparameters to obtain results with different degrees of structure preservation.

**Independent approach.** In this approach, audio and video are edited separately. For audio editing, we employed SDEdit [40] and ZETA [38], both adapted to use Stable Audio Open [12], a state-of-the-art audio generation model. For video editing, we used RAVE [26], which is based on Stable Diffusion 1.5 [44], and VACE [25], which utilizes the latest video generation model, Wan 2.1 [47]. Among the various editing tasks supported by VACE, we used the “structure transfer” in our experiments. To control the structure preservation in SDEdit and ZETA, we varied the intermediate timestep to inject the source audio information.

**Sequential approach.** In this approach, audio and video are edited in sequence. Our proposed method belongs to this category: we apply it to videos processed by RAVE and VACE and report the results (RAVE/VACE  $\rightarrow$  Ours). We varied the value of  $l_{\max}$  in Eq. 7 to control the structure preservation. We also evaluated our method with fully masked acoustic features, which completely remove source audio information from conditioning. This setting corresponds to applying a naive video-to-audio model to the edited videos (RAVE/VACE  $\rightarrow$  V2A).

### 4.3. Main results

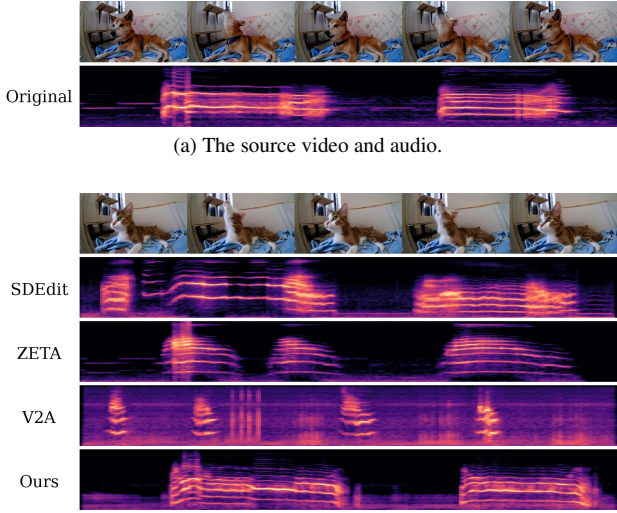
Figure 6 presents the performance of all editing methods. In both plots, the horizontal axis represents the degree of structural preservation (LPAPS). In the left plot, the vertical axis shows the audio-visual alignment between the target audio and video (IB-AV), while, in the right plot, it shows the text fidelity of the target audio (IB-TA). Figure 7 shows examples of the generated audio and video. For more examples, please refer to the supplementary materials.

Here are several observations we obtained through this experiment:

- **Benefit of sequential approach.** The sequential editing methods achieved significantly better performance in audio-visual alignment as they refer to the edited video when generating the edited audio. In contrast, the independent editing methods achieved relatively good performance in terms of text fidelity, but resulted in poor audio-visual alignment due to the lack of a mechanism for aligning edited audio and video.
- **Advantage of our method.** Simply applying video-to-audio to the edited video results in poor structure preservation, because naive video-to-audio generation cannot take the source audio into account. On the other hand, our method effectively maintains the structure of the source audio while achieving high audio-visual alignment and text fidelity.
- **Dependency on the video editing method.** Compared with VACE  $\rightarrow$  ours, the advantage of RAVE  $\rightarrow$  ours is marginal especially in terms of text fidelity. This is due to the relatively lower performance of RAVE in video editing. RAVE sometimes fails to generate a reasonable video that is well aligned with the given text prompt. In such cases, our model struggles to handle target videos and text prompts that semantically contradict each other, leading to degraded quality of the edited audio.

### 4.4. Ablation study

We also performed an ablation study to clarify how much each newly introduced component contributes to enhancing the quality of the edited audio. Specifically, we examine our method to remove the SynchFormer feature modulation (SM) described in Section 3.3, the temporal masking (TM)



(b) The target video edited by RAVE and the target audio generated by each method.

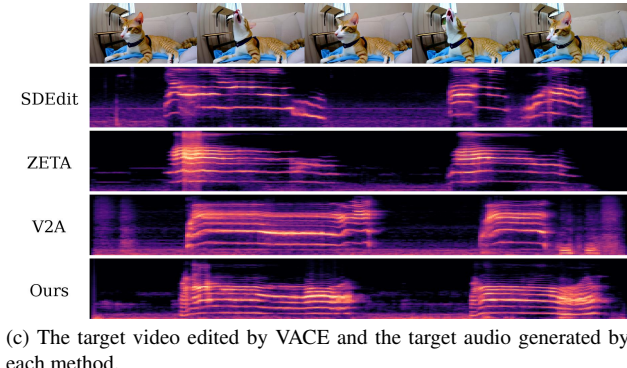


Figure 7. Examples of the generated audio and video.

in Section 3.4, and the adaptive conditioning (AC) in Section 3.5. In the case without AC, we used a fixed level of detail across all samples and varied it to control the overall degree of structure preservation.

Figure 8 shows the results of the ablation study.

- **Without SM**, the generated sounds result in similar LPAPS across various levels of detail, while achieving high performance in both audio-visual alignment and text fidelity. This indicates that modulating SynchFormer features is important for reflecting conditional acoustic information in the generated target audio.
- **Without TM**, the quality of the generated sounds degrades in both audio-visual alignment and text fidelity. This highlights that augmenting the acoustic features using temporal masking contributes to effective training of our model, even though such masking is never used during inference.
- **Without AC**, LPAPS is generally higher than with AC, while performance in audio-visual alignment and text fi-

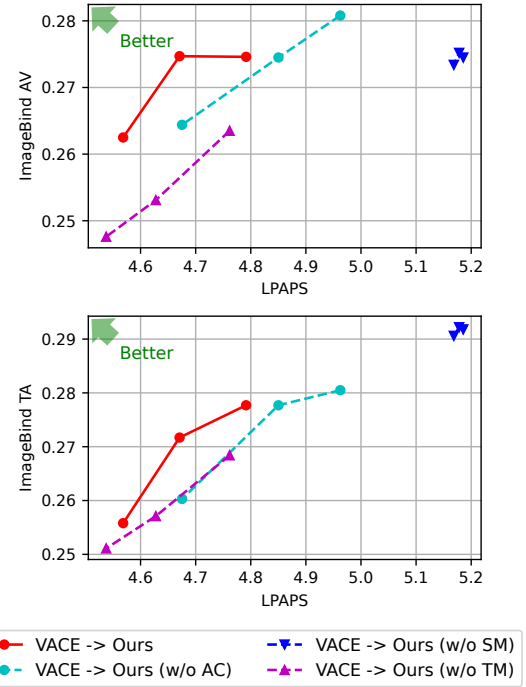


Figure 8. Ablation study.

delity remains similar. This shows that adaptively controlling the level of detail based on editability contributes to accurate preservation of the acoustic structure while maintaining the quality of the generated audio.

**Limitations.** Since our pipeline is sequential, the generation quality can be degraded by errors in video editing. As shown in Fig. 6, using more advanced video editing methods leads to better performance; thus, careful selection of the video editing method is important for our pipeline.

## 5. Conclusion

We introduced a novel audio-visual editing pipeline that first applies an existing video editing method, followed by audio editing that aligns with the video edits. To enable this, we developed a new video-to-audio model that uses the source audio as a conditional input. Our model adaptively extracts acoustic features from the source audio based on an editability score and incorporates them into the generation process to maximize retention of the original audio structure. Experimental results demonstrate that our model achieves high audio-visual alignment in the edited audio-video pairs while effectively preserving the acoustic characteristics of the source audio. As future work, we plan to extend the pipeline to support a broader range of editing tasks, such as object deletion and addition, which may require further advances in acoustic structure preservation.

## References

[1] Andreas Blattmann, Tim Dockhorn, Sumith Kulal, Daniel Mendelevitch, Maciej Kilian, Dominik Lorenz, Yam Levi, Zion English, Vikram Voleti, Adam Letts, et al. Stable video diffusion: Scaling latent video diffusion models to large datasets. *arXiv preprint arXiv:2311.15127*, 2023. 2

[2] Tim Brooks, Aleksander Holynski, and Alexei A Efros. Instructpix2pix: Learning to follow image editing instructions. In *Proceedings of the IEEE/CVF conference on computer vision and pattern recognition*, pages 18392–18402, 2023. 5

[3] Honglie Chen, Weidi Xie, Andrea Vedaldi, and Andrew Zisserman. Vggssound: A large-scale audio-visual dataset. In *ICASSP 2020-2020 IEEE International Conference on Acoustics, Speech and Signal Processing (ICASSP)*, pages 721–725. IEEE, 2020. 6

[4] Shoufa Chen, Mengmeng Xu, Jiawei Ren, Yuren Cong, Sen He, Yanping Xie, Animesh Sinha, Ping Luo, Tao Xiang, and Juan-Manuel Perez-Rua. Gentron: Diffusion transformers for image and video generation. In *Proceedings of the IEEE/CVF Conference on Computer Vision and Pattern Recognition*, pages 6441–6451, 2024. 5

[5] Ho Kei Cheng, Masato Ishii, Akio Hayakawa, Takashi Shibuya, Alexander Schwing, and Yuki Mitsuishi. Mmaudio: Taming multimodal joint training for high-quality video-to-audio synthesis. In *Proceedings of the Computer Vision and Pattern Recognition Conference*, pages 28901–28911, 2025. 1, 4, 6

[6] Nathaniel Cohen, Vladimir Kulikov, Matan Kleiner, Inbar Huberman-Spiegelglas, and Tomer Michaeli. Slicedit: Zero-shot video editing with text-to-image diffusion models using spatio-temporal slices. In *International Conference on Machine Learning*, pages 9109–9137. PMLR, 2024. 2

[7] Yuren Cong, Mengmeng Xu, Shoufa Chen, Jiawei Ren, Yanping Xie, Juan-Manuel Perez-Rua, Bodo Rosenhahn, Tao Xiang, Sen He, et al. Flatten: optical flow-guided attention for consistent text-to-video editing. In *The Twelfth International Conference on Learning Representations*, 2024. 2

[8] Google DeepMind. Veo 3. <https://deepmind.google/models/veo/>, 2025. 1

[9] Konstantinos Drossos, Samuel Lipping, and Tuomas Virtanen. Clotho: An audio captioning dataset. In *ICASSP 2020-2020 IEEE International Conference on Acoustics, Speech and Signal Processing (ICASSP)*, pages 736–740. IEEE, 2020. 6

[10] Benjamin Elizalde, Soham Deshmukh, Mahmoud Al Ismail, and Huaming Wang. Clap learning audio concepts from natural language supervision. In *ICASSP 2023-2023 IEEE International Conference on Acoustics, Speech and Signal Processing (ICASSP)*, pages 1–5. IEEE, 2023. 3

[11] Patrick Esser, Sumith Kulal, Andreas Blattmann, Rahim Entezari, Jonas Müller, Harry Saini, Yam Levi, Dominik Lorenz, Axel Sauer, Frederic Boesel, et al. Scaling rectified flow transformers for high-resolution image synthesis. In *Forty-first international conference on machine learning*, 2024. 4

[12] Zach Evans, Julian D Parker, CJ Carr, Zack Zukowski, Josiah Taylor, and Jordi Pons. Stable audio open. In *ICASSP 2025-2025 IEEE International Conference on Acoustics, Speech and Signal Processing (ICASSP)*, pages 1–5. IEEE, 2025. 7

[13] Xiang Fan, Anand Bhattad, and Ranjay Krishna. Videoshop: Localized semantic video editing with noise-extrapolated diffusion inversion. In *European Conference on Computer Vision*, pages 232–250. Springer, 2024. 2

[14] Ruiqi Gao, Emiel Hoogeboom, Jonathan Heek, Valentin De Bortoli, Kevin Patrick Murphy, and Tim Salimans. Diffusion models and gaussian flow matching: Two sides of the same coin. In *The Fourth Blogpost Track at ICLR 2025*, 2025. 2

[15] Hugo Flores García, Oriol Nieto, Justin Salamon, Bryan Pardo, and Prem Seetharaman. Sketch2sound: Controllable audio generation via time-varying signals and sonic imitations. In *ICASSP 2025-2025 IEEE International Conference on Acoustics, Speech and Signal Processing (ICASSP)*, pages 1–5. IEEE, 2025. 3

[16] Michal Geyer, Omer Bar-Tal, Shai Bagon, and Tali Dekel. Tokenflow: Consistent diffusion features for consistent video editing. In *The Twelfth International Conference on Learning Representations*, 2024. 2

[17] Deepanway Ghosal, Navonil Majumder, Ambuj Mehrish, and Soujanya Poria. Text-to-audio generation using instruction guided latent diffusion model. In *Proceedings of the 31st ACM International Conference on Multimedia*, pages 3590–3598, 2023. 2

[18] Rohit Girdhar, Alaaeldin El-Nouby, Zhuang Liu, Mannat Singh, Kalyan Vasudev Alwala, Armand Joulin, and Ishan Misra. Imagebind: One embedding space to bind them all. In *Proceedings of the IEEE/CVF conference on computer vision and pattern recognition*, pages 15180–15190, 2023. 6

[19] Amir Hertz, Ron Mokady, Jay Tenenbaum, Kfir Aberman, Yael Pritch, and Daniel Cohen-or. Prompt-to-prompt image editing with cross-attention control. In *The Eleventh International Conference on Learning Representations*, 2023. 2

[20] Jonathan Ho and Tim Salimans. Classifier-free diffusion guidance. In *NeurIPS 2021 Workshop on Deep Generative Models and Downstream Applications*, 2021. 2

[21] Jonathan Ho, Ajay Jain, and Pieter Abbeel. Denoising diffusion probabilistic models. *Advances in neural information processing systems*, 33:6840–6851, 2020. 2

[22] Vladimir Iashin and Esa Rahtu. Taming visually guided sound generation. In *British Machine Vision Conference*. BMVA Press, 2021. 6

[23] Vladimir Iashin, Weidi Xie, Esa Rahtu, and Andrew Zisserman. Syncformer: Efficient synchronization from sparse cues. In *ICASSP 2024-2024 IEEE International Conference on Acoustics, Speech and Signal Processing (ICASSP)*, pages 5325–5329. IEEE, 2024. 4

[24] Yuhang Jia, Yang Chen, Jinghua Zhao, Shiwan Zhao, Wenjia Zeng, Yong Chen, and Yong Qin. Audioeditor: A training-free diffusion-based audio editing framework. In *ICASSP 2025-2025 IEEE International Conference on Acoustics, Speech and Signal Processing (ICASSP)*, pages 1–5. IEEE, 2025. 2

[25] Zeyinzi Jiang, Zhen Han, Chaojie Mao, Jingfeng Zhang, Yulin Pan, and Yu Liu. Vace: All-in-one video creation and editing. *arXiv preprint arXiv:2503.07598*, 2025. 1, 2, 7

[26] Ozgur Kara, Bariscan Kurtkaya, Hidir Yesiltepe, James M Rehg, and Pinar Yanardag. Rave: Randomized noise shuffling for fast and consistent video editing with diffusion models. In *Proceedings of the IEEE/CVF Conference on Computer Vision and Pattern Recognition*, pages 6507–6516, 2024. 1, 2, 7

[27] Chris Dongjoo Kim, Byeongchang Kim, Hyunmin Lee, and Gunhee Kim. Audiocaps: Generating captions for audios in the wild. In *Proceedings of the 2019 Conference of the North American Chapter of the Association for Computational Linguistics: Human Language Technologies, Volume 1 (Long and Short Papers)*, pages 119–132, 2019. 6

[28] Saksham Singh Kushwaha and Yapeng Tian. Vintage: Joint video and text conditioning for holistic audio generation. In *Proceedings of the Computer Vision and Pattern Recognition Conference*, pages 13529–13539, 2025. 5

[29] Black Forest Labs. Flux. <https://github.com/black-forest-labs/flux>, 2024. 4

[30] Zitong Lan, Yiduo Hao, and Mingmin Zhao. Guiding audio editing with audio language model. *arXiv preprint arXiv:2509.21625*, 2025. 2

[31] Xirui Li, Chao Ma, Xiaokang Yang, and Ming-Hsuan Yang. Vidiome: Video token merging for zero-shot video editing. In *Proceedings of the IEEE/CVF Conference on Computer Vision and Pattern Recognition*, pages 7486–7495, 2024. 2

[32] Susan Liang, Chao Huang, Yapeng Tian, Anurag Kumar, and Chenliang Xu. Language-guided joint audio-visual editing via one-shot adaptation. In *Proceedings of the Asian Conference on Computer Vision*, pages 1011–1027, 2024. 1, 2, 3

[33] Yan-Bo Lin, Kevin Lin, Zhengyuan Yang, Linjie Li, Jianfeng Wang, Chung-Ching Lin, Xiaofei Wang, Gedas Bertasius, and Lijuan Wang. Zero-shot audio-visual editing via cross-modal delta denoising. *arXiv preprint arXiv:2503.20782*, 2025. 1, 2, 3, 6

[34] Yaron Lipman, Ricky TQ Chen, Heli Ben-Hamu, Maximilian Nickel, and Matt Le. Flow matching for generative modeling. In *11th International Conference on Learning Representations, ICLR 2023*, 2023. 2

[35] Haohe Liu, Zehua Chen, Yi Yuan, Xinhao Mei, Xubo Liu, Danilo Mandic, Wenwu Wang, and Mark D Plumbley. Audioldm: Text-to-audio generation with latent diffusion models. In *International Conference on Machine Learning*, pages 21450–21474. PMLR, 2023. 2

[36] Haohe Liu, Yi Yuan, Xubo Liu, Xinhao Mei, Qiuqiang Kong, Qiao Tian, Yuping Wang, Wenwu Wang, Yuxuan Wang, and Mark D Plumbley. Audioldm 2: Learning holistic audio generation with self-supervised pretraining. *IEEE/ACM Transactions on Audio, Speech, and Language Processing*, 32: 2871–2883, 2024. 2

[37] Shaoteng Liu, Yuechen Zhang, Wenbo Li, Zhe Lin, and Jiaya Jia. Video-p2p: Video editing with cross-attention control. In *Proceedings of the IEEE/CVF Conference on Computer Vision and Pattern Recognition*, pages 8599–8608, 2024. 2

[38] Hila Manor and Tomer Michaeli. Zero-shot unsupervised and text-based audio editing using ddpm inversion. In *International Conference on Machine Learning*, pages 34603–34629. PMLR, 2024. 2, 6, 7

[39] Xinhao Mei, Chutong Meng, Haohe Liu, Qiuqiang Kong, Tom Ko, Chengqi Zhao, Mark D Plumbley, Yuexian Zou, and Wenwu Wang. Wavcaps: A chatgpt-assisted weakly-labelled audio captioning dataset for audio-language multi-modal research. *IEEE/ACM Transactions on Audio, Speech, and Language Processing*, 32:3339–3354, 2024. 6

[40] Chenlin Meng, Yutong He, Yang Song, Jiaming Song, Jiajun Wu, Jun-Yan Zhu, and Stefano Ermon. Sdedit: Guided image synthesis and editing with stochastic differential equations. In *International Conference on Learning Representations*, 2022. 7

[41] Max Morrison, Cameron Churchwell, Nathan Pruyne, and Bryan Pardo. Fine-grained and interpretable neural speech editing. In *Proceedings of the Annual Conference of the International Speech Communication Association, INTERSPEECH*, pages 187–191, 2024. 3

[42] OpenAI. Sora 2. <https://platform.openai.com/docs/models/sora-2>, 2025. 1

[43] Ethan Perez, Florian Strub, Harm De Vries, Vincent Dumoulin, and Aaron Courville. Film: Visual reasoning with a general conditioning layer. In *Proceedings of the AAAI conference on artificial intelligence*, 2018. 4

[44] Robin Rombach, Andreas Blattmann, Dominik Lorenz, Patrick Esser, and Björn Ommer. High-resolution image synthesis with latent diffusion models. In *Proceedings of the IEEE/CVF conference on computer vision and pattern recognition*, pages 10684–10695, 2022. 2, 7

[45] Fengyuan Shi, Jiaxi Gu, Hang Xu, Songcen Xu, Wei Zhang, and Limin Wang. Bivdiff: A training-free framework for general-purpose video synthesis via bridging image and video diffusion models. In *Proceedings of the IEEE/CVF Conference on Computer Vision and Pattern Recognition*, pages 7393–7402, 2024. 2

[46] Jiaming Song, Chenlin Meng, and Stefano Ermon. Denoising diffusion implicit models. In *International Conference on Learning Representations*, 2021. 2

[47] Team Wan, Ang Wang, Baole Ai, Bin Wen, Chaojie Mao, Chen-Wei Xie, Di Chen, Fei Yu, Haiming Zhao, Jianxiao Yang, et al. Wan: Open and advanced large-scale video generative models. *arXiv preprint arXiv:2503.20314*, 2025. 2, 7

[48] Yuancheng Wang, Zeqian Ju, Xu Tan, Lei He, Zhizheng Wu, Jiang Bian, et al. Audit: Audio editing by following instructions with latent diffusion models. *Advances in Neural Information Processing Systems*, 36:71340–71357, 2023. 2

[49] Yongqi Wang, Wenxiang Guo, Rongjie Huang, Jiawei Huang, Zehan Wang, Fuming You, Ruiqi Li, and Zhou Zhao. Frieren: Efficient video-to-audio generation network with rectified flow matching. *Advances in Neural Information Processing Systems*, 37:128118–128138, 2024. 4

[50] Jay Zhangjie Wu, Yixiao Ge, Xintao Wang, Stan Weixian Lei, Yuchao Gu, Yufei Shi, Wynne Hsu, Ying Shan, Xiaohu Qie, and Mike Zheng Shou. Tune-a-video: One-shot tuning of image diffusion models for text-to-video generation. In *Proceedings of the IEEE/CVF international conference on computer vision*, pages 7623–7633, 2023. 2

[51] Manjie Xu, Chenxing Li, Duzhen Zhang, Dan Su, Wei Liang, and Dong Yu. Prompt-guided precise audio editing

with diffusion models. In *International Conference on Machine Learning*, pages 55126–55143. PMLR, 2024. [2](#)

[52] Zhuoyi Yang, Jiayan Teng, Wendi Zheng, Ming Ding, Shiyu Huang, Jiazheng Xu, Yuanming Yang, Wenyi Hong, Xiaohan Zhang, Guanyu Feng, et al. Cogvideox: Text-to-video diffusion models with an expert transformer. In *The Thirteenth International Conference on Learning Representations*, 2025. [2](#)

[53] Yanming Zhang, Jun-Kun Chen, Jipeng Lyu, and Yu-Xiong Wang. V2edit: Versatile video diffusion editor for videos and 3d scenes. *arXiv preprint arXiv:2503.10634*, 2025. [2](#)

[54] Yixuan Zhu, Wenliang Zhao, Ao Li, Yansong Tang, Jie Zhou, and Jiwen Lu. Flowie: Efficient image enhancement via rectified flow. In *Proceedings of the IEEE/CVF Conference on Computer Vision and Pattern Recognition*, pages 13–22, 2024. [4](#)